Avoided-Level-Crossing Spectroscopy with Dressed Matter Waves

André Eckardt[1,*] and Martin Holthaus[2]

[1]ICFO-Institut de Ciències Fotòniques, E-08860 Castelldefels (Barcelona), Spain

[2]Institut für Physik, Carl von Ossietzky Universität, D-26111 Oldenburg, Germany

(Received 5 September 2008; published 12 December 2008)

We devise a method for probing resonances of macroscopic matter waves in shaken optical lattices by monitoring their response to slow parameter changes, and show that such resonances can be disabled by particular choices of the driving amplitude. The theoretical analysis of this scheme reveals far-reaching analogies between dressed atoms and time periodically forced matter waves.

DOI: 10.1103/PhysRevLett.101.245302 PACS numbers: 67.85.Hj, 03.75.Lm, 42.50.Hz

Recently, it has been demonstrated experimentally that a macroscopic matter wave of ultracold bosonic atoms confined in an optical lattice can be controlled in a systematic manner by strong, off-resonant time-periodic forcing: Under suitably selected conditions, "shaking" the lattice with kilohertz frequencies mainly effectuates a modification of the tunneling matrix element connecting adjacent lattice sites. In the regime of weak interaction, this phenomenon has been inferred from the expansion of a Bose-Einstein condensate in a one-dimensional lattice geometry [1]. A subsequent experiment [2] utilizes the reduction of the tunneling matrix element to augment the relative importance of interparticle repulsion, such that the quantum phase transition from a superfluid to a Mott-insulator [3,4] is induced by adiabatically varying the amplitude of the driving force [5].

These landmark experiments [1,2] clearly confirm that there are efficient control mechanisms for ultracold atomic gases resulting from time-periodic modulation. The situation encountered here is akin to the dressed-atom approach: An atom in a laser field becomes "dressed" by that field and changes its behavior [6]. Similarly, a many-body matter wave becomes dressed in response to time-periodic forcing and acquires properties which the unforced, bare matter wave did not have.

A system of ultracold bosonic atoms in a shaken, sufficiently deep one-dimensional optical lattice is described, in the frame of reference comoving with the lattice, by the driven Bose-Hubbard model defined by the Hamiltonian $\hat{H}(t) = \hat{H}_{\rm tun} + \hat{H}_{\rm int} + \hat{H}_{\rm drive}(t)$ [5,7]. With $\hat{b}_\ell$ and $\hat{n}_\ell = \hat{b}_\ell^\dagger \hat{b}_\ell$ denoting the bosonic annihilation and the number operator for the Wannier state located at the site labeled by $\ell = 1, 2, \ldots, M$, one has $\hat{H}_{\rm tun} \equiv -J \sum_{\ell=1}^{M-1} (\hat{b}_\ell^\dagger \hat{b}_{\ell+1} + \hat{b}_{\ell+1}^\dagger \hat{b}_\ell)$, where the positive hopping parameter J implements the kinetics, assumed to be exhausted by tunneling between adjacent sites. Moreover, $\hat{H}_{\rm int} \equiv \frac{U}{2} \sum_{\ell=1}^{M} \hat{n}_\ell(\hat{n}_\ell - 1)$ with positive interaction parameter U describes the repulsion of particles occupying the same site. Finally, $\hat{H}_{\rm drive}(t) \equiv K_\omega \cos(\omega t) \sum_{\ell=1}^{M} \ell \hat{n}_\ell$ models time-periodic forcing with amplitude K_ω and angular frequency ω. With the particle number fixed to N, the filling n is given by the ratio $n \equiv N/M$.

As witnessed by the experiments [1,2], in a time-averaged sense, the *driven* system governed by $\hat{H}(t)$ behaves similar to a system described by the effective, *time-independent* Hamiltonian $\hat{H}_{\rm eff} \equiv \mathcal{J}_0(K_\omega/\hbar\omega)\hat{H}_{\rm tun} + \hat{H}_{\rm int}$, which means that the effect of the time-periodic force is captured by replacing the tunneling matrix element J by $J_{\rm eff} \equiv \mathcal{J}_0(K_\omega/\hbar\omega)J$, with $\mathcal{J}_0$ denoting the ordinary Bessel function of order zero. This modification of the hopping matrix element is a hallmark of driven quantum tunneling [8]; it has been cleanly observed for single-particle tunneling in strongly driven double-well potentials [9]. While it becomes exact for a single particle on a one-dimensional lattice endowed with nearest-neighbor coupling [10], the dynamics are considerably more involved in the many-body case described by the driven Bose-Hubbard model. Because of the manifold ways to create excitations in the many-body system, the $\hat{H}_{\rm eff}$-description is endangered by a multitude of resonances, and holds approximately only when $\hbar\omega$ is large compared to both energy scales which characterize the undriven system, U and nJ [5,11,12]. To further explore the newly emerging notion of adiabatic control of driven macroscopic matter waves [2], it is now of great importance to study such resonances in detail: When do they occur, how strong are they, are they detrimental to coherent control, or can they, perhaps, even be exploited? These questions mark the scope of the present Letter. By means of numerical simulations for small systems, we first outline an experimentally feasible detection scheme which allows one to locate major excitation channels in parameter space, and to probe their strengths. We also demonstrate that the strength of such excitation channels again is subject to coherent control: A resonance can be completely quenched by an appropriate choice of the driving amplitude. In a second step, we make closer contact between the dressed-atom picture and the driven matter waves considered here by studying their quasienergy spectrum. In the final third step, we explain our findings quantitatively by means of perturbation theory for Floquet states.

Consider the following scenario: A system conforming to the undriven Bose-Hubbard model $\hat{H}_{\rm tun} + \hat{H}_{\rm int}$ is prepared in its ground state for $U/J = 0.1$. Then, a drive $\hat{H}_{\rm drive}(t)$ is switched on, with an amplitude increasing linearly in time, and a high frequency $\hbar\omega/J = 20$. Since this drive is sufficiently off-resonant, one expects the system to adiabatically follow the ground state of $\hat{H}_{\rm eff}$. After the working amplitude K_ω has been reached, it is held constant. Then, the interaction parameter U is ramped up at constant rate $\eta \equiv \dot{U}T/J$ (with $T = 2\pi/\omega$) into the regime where resonances should make themselves felt. In a laboratory experiment, this can be done, e.g., by increasing the transversal confinement used to create the effective one-dimensional geometry. We have simulated this protocol for a small system with $N = M = 7$. In Fig. 1, we plot the squared overlap $P_{\rm eff}(t) = |\langle\psi_0^{(\rm eff)}|\psi(t)\rangle|^2$ of the system's true state $|\psi(t)\rangle$, obtained by solving the full time-dependent Schrödinger equation governed by $\hat{H}(t)$, and the ground states $|\psi_0^{(\rm eff)}\rangle$ of the corresponding instantaneous operators $\hat{H}_{\rm eff}$. Figure 1(a) is obtained for $K_\omega/\hbar\omega = 2.5$. As expected, $P_{\rm eff}$ stays close to unity even when U becomes large, thus validating the $\hat{H}_{\rm eff}$-description, until at $U/\hbar\omega \approx 2/3$, it decreases suddenly; the drop is the more pronounced, the lower the rate η. This abrupt decrease signals resonant excitation. Experimentally, such resonant excitation can be detected by time-of flight absorption imaging. It is indicated by a loss of contrast of the sharply peaked structures visible in either the single-particle momentum distribution [4] if the system is in the superfluid regime (which may be reached by a further adiabatic parameter variation), or in the two-particle momentum correlations [13,14] if the system is in the Mott-insulator regime. Interestingly, when choosing the particular driving amplitude $K_\omega/\hbar\omega = 3.4$, this excitation channel is closed, and another one at $U/\hbar\omega \approx 1$ appears in Fig. 1(b). This second resonance is stronger than the first one, since the drop is fully developed already for larger η. We conclude: (i) $\hat{H}_{\rm eff}$ describes the system up to surprisingly large interaction strengths U; (ii) the excitation observed at $U/\hbar\omega \approx 2/3$ in Fig. 1(a), and at $U/\hbar\omega \approx 1$ in Fig. 1(b), cannot be ascribed to a deviation from adiabatic following on the level of $\hat{H}_{\rm eff}$, since the degree of excitation increases with *decreasing* parameter variation rate η; (iii) a resonance can be disabled by adjusting the driving amplitude. Thus, by applying this or a similar protocol, both the locations and the strengths of resonant excitation channels can be probed.

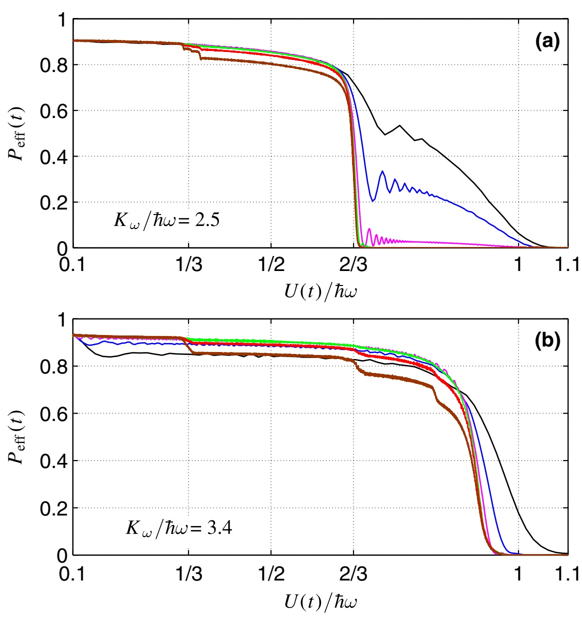

FIG. 1 (color online). Exact time evolution of $N = 7$ particles on $M = 7$ lattice sites. Starting in the ground state at interaction strength $U/J = 0.1$, a drive of frequency $\hbar\omega/J = 20$ has been linearly ramped up within 50 cycles $T = 2\pi/\omega$ to the working amplitude K_ω, before U is increased at various rates $\eta \equiv \dot{U}T/J = 0.3$, 0.1, 0.03, 0.01, 0.003, 0.001. We plot the squared overlap $P_{\rm eff}(t)$ of the instantaneous ground state of $\hat{H}_{\rm eff}$ with the actual time-evolved state versus $U(t)/\hbar\omega$ at integer t/T. For large $U(t)/\hbar\omega$, $P_{\rm eff}$ decreases with decreasing η; the lower η, the steeper the drop. For $K_\omega/\hbar\omega = 2.5$, there is strong resonant excitation at $U/\hbar\omega = 2/3$ (a). For $K_\omega/\hbar\omega = 3.4$, this resonance is quenched, and another one around $U/\hbar\omega = 1$ becomes active (b).

We now shed light on the physics underlying this detection scheme, and provide an appropriate theoretical framework. Recall that the dressed-atom approach deals with atoms interacting with a quantized mode of a radiation field. Accordingly, the energy level diagram of the combined system features identical copies of groups of levels displaced against each other by the photon energy $\hbar\omega$ [6]. An analogous picture for dressed matter waves driven by a classical time-periodic force is obtained by quantum Floquet theory [15,16]: Given the Hamiltonian $\hat{H}(t) = \hat{H}(t+T)$, one defines the quasienergy operator $\hat{Q} \equiv \hat{H}(t) - i\hbar\partial_t$ which acts in the product space $\mathcal{H} \otimes \mathcal{T}$ made up from the physical state space $\mathcal{H}$ and the space $\mathcal{T}$ of T-periodic functions, and solves the eigenvalue problem $\hat{Q}|u(t)\rangle\rangle = \varepsilon|u(t)\rangle\rangle$. Because of the periodic boundary conditions in time, the solutions have the form $|u_{\nu,m}(t)\rangle\rangle \equiv |u_{\nu,0}(t)\rangle\rangle \exp(im\omega t)$, with $\omega = 2\pi/T$ and $m = 0, \pm1, \pm2, \ldots$; the label ν is chosen such that $|u_{\nu,0}(t)\rangle\rangle$ connects to the ν-th energy eigenstate when the driving force vanishes. Hence, the eigenvalues $\varepsilon_{\nu,m} \equiv \varepsilon_{\nu,0} + m\hbar\omega$, called quasienergies, repeat themselves with period $\hbar\omega$ on the energy axis; each state ν placing one copy in each "Brillouin zone" of width $\hbar\omega$. Going back to the actual state space $\mathcal{H}$, the states $|\psi_\nu(t)\rangle = |u_{\nu,m}(t)\rangle\rangle \times \exp(-i\varepsilon_{\nu,m}t/\hbar)$ form a complete set of solutions to the time-dependent Schrödinger equation.

Figure 2 shows a part of the quasienergy spectrum belonging to a small driven Bose-Hubbard system ($N = M = 5$) with $\hbar\omega/J = 20$ and $K_\omega/\hbar\omega = 2$ versus U/J. Its basic structure, shown in subplot (a), can be understood as a superposition of copies of the energy spectrum of $\hat{H}_{\rm eff}$,

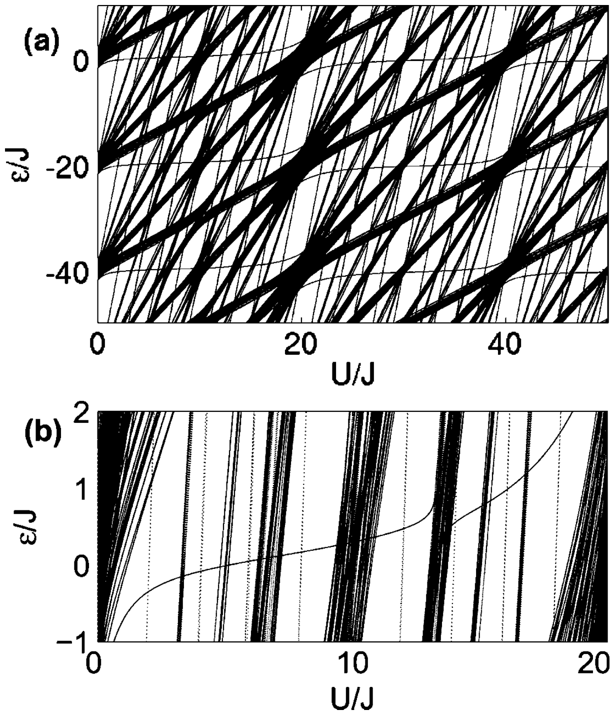

FIG. 2. (a) Quasienergy spectrum of a driven Bose-Hubbard system with $N = M = 5$, $\hbar\omega/J = 20$, and $K_\omega/\hbar\omega = 2$ versus U/J. Bands with different slopes belong to different types of particle-hole excitations of $\hat{H}_{\rm eff}$. Resonant coupling of such bands results in avoided crossings. The isolated quasienergy level, highlighted in (b), emerges from the ground state of the undriven system. Clearly visible are the avoided crossings at $U/\hbar\omega \approx 2/3$ ($U/J \approx 13$) and $U/\hbar\omega \approx 1$ ($U/J \approx 20$) which have been detected dynamically in Fig. 1, whereas there are no avoided crossings at 1/3 and 1/2.

shifted against each other by integer multiples of $\hbar\omega$. The spectrum of $\hat{H}_{\rm eff}$ possesses bands, made up from various types of particle-hole excitations with energies roughly corresponding to integer multiples of U, clearly identifiable through their slopes. While in Fig. 2(a) quasienergy levels belonging to different copies of the $\hat{H}_{\rm eff}$-spectrum hardly "notice" each other for interaction strengths U/J much smaller than $\hbar\omega/J = 20$, there are pronounced avoided crossings when U/J becomes comparable to $\hbar\omega/J$, prominently exemplified by the complex patterns which appear when U/J is an integer multiple of $\hbar\omega/J$. Such avoided crossings indicate resonances which emerge if eigenstates of $\hat{H}_{\rm eff}$ are energetically separated by an integer multiple of $\hbar\omega$; their size quantifies the strength of resonant coupling and determines the degree of deviation from the $\hat{H}_{\rm eff}$-description.

Figure 2(b) shows a detail of Fig. 2(a), focusing on one of the quasienergy copies corresponding to the ground state of $\hat{H}_{\rm eff}$. After separating from the bands of excited states with increasing U/J, thus indicating the superfluid to Mott-insulator transition [2,5], this level crosses several bands associated with different copies of the $\hat{H}_{\rm eff}$-spectrum without being notably affected, until it undergoes a wide avoided crossing with such a band at $U/J \approx \frac{2}{3}\hbar\omega/J \approx 13$, and subsequently an even wider one around $U/J \approx \hbar\omega/J = 20$. These avoided crossings explain the excitation observed in Fig. 1: The dynamical detection scheme illustrated by that figure relies on the adiabatic principle for Floquet states [12]. With increasing U, the state $|\psi(t)\rangle$ adjusts itself to the slowly changing parameter and thus follows the quasienergy level corresponding to the ground state of $\hat{H}_{\rm eff}$, until it reaches an avoided crossing too wide to be passed *diabatically.* Then, an incomplete Landau-Zener transition to the anticrossing state excites the system. According to Landau-Zener estimates, and in agreement with the simulations depicted in Fig. 1, the excitation probability increases exponentially with both the width of the anticrossing and decreasing parameter speed. Thus, the method of detecting resonances in dressed matter waves by monitoring their response to slow parameter changes can be regarded as a kind of avoided-level-crossing spectroscopy.

Note that in contrast to the regime of linear response, suitable for probing properties of the undriven system, here we consider the excitation of a system which has already been strongly modified by the driving force, in a manner described by $\hat{H}_{\rm eff}$. Moreover, besides the wide, "active" avoided quasienergy crossings there also is a host of tiny avoided crossings, reflecting the high density of quasienergies in each Brillouin zone so that effectively adiabatic dynamics on the level of $\hat{H}_{\rm eff}$ actually includes fully diabatic Landau-Zener tunneling through these narrow anticrossings. In an infinitely large system with a truly dense quasienergy spectrum, the existence of a well-defined adiabatic limit cannot, thus, be expected [17]. However, realistic parameter variations take place on finite time scales, in all likelihood making the system "blind" against such small features of the spectrum.

We now formalize our reasoning. For each admissible set $\{n_\ell\}$ of site-occupation numbers, we employ the usual Fock states $|\{n_\ell\}\rangle \equiv \prod_\ell (n_\ell!)^{-(1/2)}(\hat{b}_\ell^\dagger)^{n_\ell}|\text{vacuum}\rangle$ for constructing an orthonormal basis of Floquet-Fock states $|\{n_\ell\},\tilde{m}\rangle\rangle \equiv |\{n_\ell\}\rangle \exp[-i\frac{K_\omega}{\hbar\omega}\sin(\omega t)\sum_\ell \ell n_\ell]\exp(i\tilde{m}\omega t)$ in $\mathcal{H}\otimes\mathcal{T}$, with $\tilde{m}$ serving as "photon" index for distinguishing different Brillouin zones. Invoking the scalar product $\langle\langle\cdot|\cdot\rangle\rangle \equiv \frac{1}{T}\int_0^T dt\langle\cdot|\cdot\rangle$, the quasienergy operator $\hat{Q} \equiv \hat{Q}_0 + \hat{Q}_1$ of the driven Bose-Hubbard model possesses the matrix elements

$$\langle\langle\{n'_\ell\},\tilde{m}'|\hat{Q}_0|\{n_\ell\},\tilde{m}\rangle\rangle = \delta_{\tilde{m}',\tilde{m}}\langle\{n'_\ell\}|(\tilde{m}\hbar\omega + \hat{H}_{\rm int} + j_0\hat{H}_{\rm tun})|\{n_\ell\}\rangle,$$

$$\langle\langle\{n'_\ell\},\tilde{m}'|\hat{Q}_1|\{n_\ell\},\tilde{m}\rangle\rangle = (1-\delta_{\tilde{m}',\tilde{m}})j_{s(\tilde{m}-\tilde{m}')}\langle\{n'_\ell\}|\hat{H}_{\rm tun}|\{n_\ell\}\rangle,$$

where $j_\nu \equiv \mathcal{J}_\nu(K_\omega/\hbar\omega)$ indicates the Bessel function of order ν evaluated at $K_\omega/\hbar\omega$, and $s \equiv \sum_\ell \ell(n_\ell - n'_\ell)$, giving $s = +1$ ($s = -1$) if $\hat{H}_{\rm tun}$ transfers one particle by one site to the left (right) [11,12]. This splitting of the quasienergy operator is performed such that $\hat{Q}_0$ acts within each

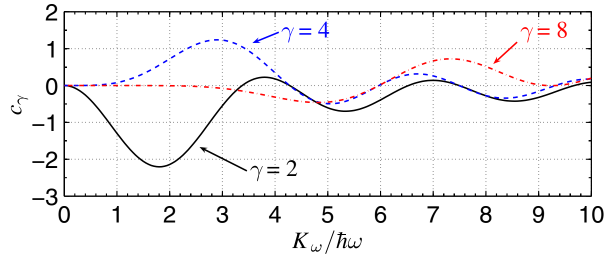

FIG. 3 (color online). Coupling strength c_γ of simultaneous resonant excitation of two particle-hole pairs with the two extra particles located at the same site, evaluated at $U = \gamma\hbar\omega/3$.

subspace with fixed "photon" number $\tilde{m}$ in a manner conforming to $\hat{H}_{\rm eff}$; whereas $\hat{Q}_1$ describes the coupling between these subspaces.

Let us assume that U is comparable to $\hbar\omega$ while $\hbar\omega \gg nJ$, and treat $\hat{Q}_1$ by perturbation theory. For $U \gg n|J_{\rm eff}|$, the ground state of $\hat{H}_{\rm eff}$ is approximately given by the extreme Mott-insulator state $|{\rm MI}\rangle \equiv |\{n_\ell = n\}\rangle$ with n particles localized at each site. Excited states differ from $|{\rm MI}\rangle$ by particle-hole excitations of energy U; these excitations form bands with widths on the order of $\sim n|J_{\rm eff}|$ due to tunneling of the particles and holes "on top" of $|{\rm MI}\rangle$. Thus, near $U = \alpha\hbar\omega$ with integer $\alpha = 1, 2, \ldots$, the drive is resonant with respect to the creation of a single particle-hole pair; eigenstates of $\hat{Q}_0$ differing from $|{\rm MI}\rangle$ by one particle-hole pair and α "photons" are degenerate with $|{\rm MI}\rangle$ and couple directly (i.e., in first order) via $\hat{Q}_1$ by matrix elements of size $-\sqrt{n(n+1)}Jj_{s\alpha}$. This coupling leads to the large avoided band or level crossings visible in Fig. 2 at U/J close to 20 and 40.

In second order, the simultaneous creation of two particle-hole pairs via (quasi-)energetically distant intermediate states is taken into account. Intriguingly, second-order coupling between states differing from $|{\rm MI}\rangle$ by β "photons" and two separate particle-hole excitations of total energy $2U$, expected near $U = \beta\hbar\omega/2$ with $\beta = 1, 3, 5, \ldots$ (omitting first-order resonances), vanishes completely due to destructive interference between paths involving different intermediate states. This explains why there is *no* avoided crossing at $U/J \approx 10$ in Fig. 2. However, there are nonvanishing second-order processes creating two *overlapping* particle-hole pairs, having two particles or holes sitting at the same site. Assuming unit filling $n = 1$, the only possibility is to place both particles at the same site, costing the excitation energy $3U$. For such excitations near $U = \gamma\hbar\omega/3$ with $\gamma = 1, 2, 4, 5, \ldots$, we find coupling constants $c_\gamma J^2 n\sqrt{(n+1)(n+2)}/\hbar\omega$ with strengths $c_\gamma \equiv \frac{1}{2}[\sum_{\tilde{m}'=-\infty}^{\infty}(j_{(\gamma+\tilde{m}')}j_{\tilde{m}'} + j_{-(\gamma+\tilde{m}')}j_{-\tilde{m}'})] \times [(2U/\hbar\omega - \gamma - \tilde{m}')^{-1} - (U/\hbar\omega + \tilde{m}')^{-1}]$ which vanish for odd γ. The plot of c_γ depicted in Fig. 3 testifies that these strengths depend in an oscillating manner on the driving amplitude. In particular, it is possible to adjust that amplitude such that the resonant coupling strength vanishes. For instance, the zero of c_2 at $K_\omega/\hbar\omega \approx 3.4$ is the reason for the resonance quenching illustrated in Fig. 1. In νth order, coupling matrix elements generally are $\sim nJ(nJ/\hbar\omega)^{\nu-1}$; however, we have hardly noticed third-order effects in our numerical simulations. Thus, degenerate-state perturbation theory in $\mathcal{H} \otimes \mathcal{T}$ systematically uncovers the hierarchy of resonances which, in a system with slowly changing parameters, become observable order by order with decreasing parameter speed.

To conclude, we have outlined a scheme for probing resonances which endanger the adiabatic control of macroscopic matter waves achievable through time-periodic forcing [2]. The theoretical analysis of this scheme reveals far-reaching conceptual similarities between dressed atoms and dressed matter waves in shaken optical lattices, thus opening up wide new grounds between quantum optics and matter-wave physics.

We thank O. Morsch for many discussions of the experiments [1,2]. A. E. is grateful to M. Lewenstein for kind hospitality at ICFO-Institut de Ciències Fotòniques, and acknowledges a Feodor Lynen research grant from the Alexander von Humboldt foundation.

*andre.eckardt@icfo.es

[1] H. Lignier, C. Sias, D. Ciampini, Y. Singh, A. Zenesini, O. Morsch, and E. Arimondo, Phys. Rev. Lett. **99**, 220403 (2007).
[2] A. Zenesini, H. Lignier, D. Ciampini, O. Morsch, and E. Arimondo, arXiv:0809.0768.
[3] M. P. A. Fisher, P. B. Weichman, G. Grinstein, and D. S. Fisher, Phys. Rev. B **40**, 546 (1989).
[4] I. Bloch, J. Dalibard, and W. Zwerger, Rev. Mod. Phys. **80**, 885 (2008).
[5] A. Eckardt, C. Weiss, and M. Holthaus, Phys. Rev. Lett. **95**, 260404 (2005).
[6] C. Cohen-Tannoudji, J. Dupont-Roc, and G. Grynberg, *Atom-Photon Interactions: Basic Processes and Applications* (Wiley-VCH, Weinheim, 1998).
[7] C. E. Creffield and T. S. Monteiro, Phys. Rev. Lett. **96**, 210403 (2006).
[8] M. Grifoni and P. Hänggi, Phys. Rep. **304**, 229 (1998).
[9] E. Kierig, U. Schnorrberger, A. Schietinger, J. Tomkovic, and M. K. Oberthaler, Phys. Rev. Lett. **100**, 190405 (2008).
[10] M. Holthaus and D. Hone, Phys. Rev. B **47**, 6499 (1993).
[11] A. Eckardt and M. Holthaus, EPL **80**, 50004 (2007).
[12] A. Eckardt and M. Holthaus, J. Phys: Conference Series **99**, 012007 (2008).
[13] E. Altman, E. Demler, and M. D. Lukin, Phys. Rev. A **70**, 013603 (2004).
[14] S. Fölling, F. Gerbier, A. Widera, O. Mandel, T. Gericke, and I. Bloch, Nature (London) **434**, 481 (2005).
[15] J. H. Shirley, Phys. Rev. **138**, B979 (1965).
[16] H. Sambe, Phys. Rev. A **7**, 2203 (1973).
[17] D. W. Hone, R. Ketzmerick, and W. Kohn, Phys. Rev. A **56**, 4045 (1997).